Pure Appl. Chem., Vol. 76, No. 1, pp. 79–89, 2004.

Inelastic X-ray scattering and high-frequency dynamics of molecular liquids*

E. Pontecorvo[1], R. Di Leonardo[1], C. Masciovecchio[2], G. Ruocco[1], B. Ruzicka[1], T. Scopigno[1,‡], and F. Sette[3]

[1]*Dipartimento di Fisica and INFM, Universita di Roma "La Sapienza", I-00185, Roma, Italy;* [2]*Sincrotrone Trieste, Area Science Park, I-34012, Trieste, Italy;* [3]*European Synchrotron Radiation Facility, B.P. 220 F-38043 Grenoble, Cedex, France*

Abstract: The recently developed inelastic X-ray scattering technique opens a new kinematic region at the observation of molecular liquids vibrational dynamics over the length scales of the interparticle separation. We illustrate the capabilities of this powerful technique through the results obtained from liquid glycerol. A detailed analysis of the high-frequency vibrational dynamics of this system at ambient temperature is reported. New results in the study of structural relaxational dynamics in the high-temperature range (up to $T = 560$ K) are also discussed.

INTRODUCTION

When we leave the time and length scales appropriate for the description of a liquid as a continuous medium and therefore from the applicability of the strict hydrodynamic theory, our understanding must face the difficulties due to the lack of translational symmetry and to the approaching time scales characteristic of several specific relaxation processes. On these scales, a satisfactory theoretical description of the dynamical problem is still missing, and this characterization has motivated many theoretical and experimental efforts. From both these points of view, an important observable is represented by the dynamical structure factor, $S(Q,\omega)$. It is defined as the Fourier transform in space and time of the particles' density pair correlation function, and exhibits features in both the energy E and the wavevector Q, which correspond to the characteristic excitations of the system

$$S(Q,E) = \frac{1}{2\pi}\frac{1}{N}\int dt\, e^{i\omega t} \sum_{m,n} \left\langle e^{i\boldsymbol{Q}\cdot\boldsymbol{r}_m(t)} e^{-i\boldsymbol{Q}\cdot\boldsymbol{r}_n(0)} \right\rangle \tag{1}$$

with N the number of particles in the system whose position at time t are $\boldsymbol{r_n}(t)$ ($n = 1...N$). If we now consider the medium as a continuum and over a time scale long enough that the system can be assumed to be in thermodynamical equilibrium (i.e., the limit $Q \to 0$), the hydrodynamic theory provides us an explicit expression for $S(Q,E)$ [1]. The spectrum comprises three lines, referred to as the Brillouin triplet, which are centered at $E = 0$ and $E = \pm\hbar c_0 Q$, and correspond respectively to the entropy fluctuations, and to the compression wave propagating with the adiabatic sound velocity c_0. The two lines at $E = \pm\hbar c_0 Q$ correspond to the energy loss and energy gain and have a width proportional to the longitudinal viscosity and Q^2-dependent. The sound attenuation mechanism is therefore mainly due to viscosity effects, and the energy is dissipated through the structural rearrangements. This simple view is not

*Lecture presented at the European Molecular Liquids Group (EMLG) Annual Meeting on the Physical Chemistry of Liquids: Novel Approaches to the Structure, Dynamics of Liquids: Experiments, Theories, and Simulation, Rhodes, Greece, 7–15 September 2002. Other presentations are published in this issue, pp. 1–261.

‡Corresponding author

a priori expected to hold if we now consider distances comparable to those that characterize structural correlations among particles, and times comparable to the lifetime of these correlations. In this intermediate scale, one expects to observe a large modification of the dynamics when the considered time scales are either much larger or much shorter than those associated to the relaxation of a spontaneous density fluctuation toward its equilibrium state. The Brillouin light-scattering experiments [2], in systems with a very long structural relaxation time (glass-forming liquids) have shown that when the explored frequency range matches the inverse of these characteristic time scales, the system passes from the previously described liquid-like regime to a solid-like one. This transition is marked by the modification of the speed of sound from the hydrodynamic value c_0 to higher value c_∞, when the excitation frequency $E/\hbar$ is comparable with $1/\tau$: such a dispersion of velocity is typically observed changing the thermodynamic state of the system (temperature), and therefore τ. The width of the Brillouin lines is also changed in this transition as the dissipation through structural rearrangement is frozen; however, the peak still presents a finite width due to different dumping mechanisms: the origin of a finite lifetime for plane wave lies now both in the presence of anharmonicity effects both in the fact that Q is no more a good quantum number due to the topological disorder of liquid structure. But what about this collective dynamics picture when we go toward Q values approaching the first maximum Q_m of the static structure factor, $S(Q)$? Is the propagation of collective modes still possible? And how does the relaxation influence the spectra if it lies at a much faster time scale? Numerical simulations give an answer to this questions: the continuous evolution from the Brillouin triplet in the hydrodynamic limit toward a more complex three peaks structure that seems to survive up to higher Q values, has been studied by a large number of molecular dynamics (MD) simulations. For example, in the case of simple monoatomic fluids, this evolution has been analyzed by several MD studies performed with both hard spheres [3] and Lennard–Jones potentials [4].

On the other side, the extension to larger Q and E values up to $Q \approx Q_m$, has been experimentally more difficult, until the development of inelastic X-ray scattering (IXS) spectroscopy with meV energy resolution. The highly developed inelastic neutron scattering (INS) technique, in fact, cannot be easily applied at Q transfers smaller than 10 nm^{-1} on typical liquid systems because the required energy transfer for the excitation of an acoustic mode are often too large for this probe. This limitation is intrinsic to the kinematics of the scattering process: it is, indeed, not possible, to study acoustic excitations propagating with a speed of sound, c, using a probe particle with a speed c_i smaller than c. These restrictions of the accessible kinematic range are not particularly relevant in the studies of crystalline samples with neutron spectroscopies. Here, the translation invariance allows us to study the acoustic excitations in high-order Brillouin zones, and this overcomes the mentioned limits on phonon branches with steep dispersions. On the contrary, the situation is very different for topologically disordered systems: in these systems, in fact, the absence of periodicity imposes that the acoustic excitations must be measured at small momentum transfers to follow, as just said, the evolution of the dynamical structure factor from the Brillouin triplet to the higher Q disorder influenced complex line shape.

INELASTIC X-RAY SCATTERING WITH *MILLI*-ELECTRON-VOLT ENERGY RESOLUTION

The choice to overcome the discussed limitations clearly falls to the use of a nonmassive probe as X-photons but the price to pay for realizing this purpose is high: contrary to X-rays, the phase space of thermal neutrons matches very well that of phonon-like collective excitations; the energy of neutrons with wavelengths of the order of interparticle distances is about 100 meV, and this value is comparable to the energies of phonons with wavelengths in the nanometer range, while a photon with the same momentum has an energy of ≈10 keV. This implicates that we need an energy resolution $\Delta E/E \approx 10^{-7}$.

However, if we take care to be sufficiently far away from a photoabsorption edge of a core-line in the investigated system, the X-ray scattering cross-section takes the simple Thomson expression:

$$\frac{\partial^2\sigma(E,\Omega)}{\partial\Omega\partial E} = r_o^2\left(\varepsilon_i\cdot\varepsilon_f\right)^2\frac{k_f}{k_i}|f(Q)|^2\,S(Q,E). \tag{2}$$

where $f(Q)$ is the form factor and as in a typical scattering experiment in which an initial photon of energy E_i, momentum $\mathbf{k}_i$ and polarization ω_i is diffused into a final state of energy E_f, momentum $\mathbf{k}_f$ and polarization ω_f, $E = E_f - E_i$ and $Q = |\mathbf{k}_f - \mathbf{k}_i|$ are the exchanged energy and momentum. This expression is very close to neutrons cross-section revealing the density fluctuations information in its being proportional to the $S(Q,\omega)$. Moreover, the classical electron radius r_o has a value comparable to the neutrons coupling constant. The expression (2) simply holds under (i) the adiabatic approximation, working very well when the exchanged energies are small with respect to the excitation energies of electrons in bound core states (considering the energy of typical phonon excitations, this is indeed the case in basically any atom), and (ii) the assumption to consider a situation in which the electronic part of the total wavefunction is not changed by the scattering process.

Despite that the coupling intensity of the probe with the matter is comparable, as we just stressed, in both INS and IXS techniques, we must take care that the total absorption cross-section of X-rays of 10 keV energy is mainly due to the photoelectric absorption process ($\propto Z^4$) and not to the Thomson scattering process ($\propto Z^2$). Consequently, the Thomson scattering channel is not very efficient for system with high Z. Moreover, the rapid decrease of the atomic form factor $f(Q)$ with increasing Q is responsible for a further drastic reduction of the scattering cross-section, already at relatively small momentum transfer values.

Therefore, the implementation of an IXS experiment must solve the main problem to reach the high-resolution $\Delta E/E \approx 10^{-7}$ having a residual flux of photons high enough to be able to observe an inelastic signal in spite of the low scattering rates. In the following, we are going to illustrate how these difficulties have been overcome on the first high-resolution spectrometer built-up on the beamline ID16 at the European Synchrotron Radiation Facility in Grenoble (France).

In Fig. 1, we report the main optical elements of the ESRF IXS beamline. The instrument, a triple axis spectrometer, has as first axis the monochromator crystal, whose role is to determine the energy, E_i, of the incident photons. The second axis is the one devoted to the scattering process, where one selects the scattering angle θ_s, and therefore, the exchanged momentum: for the energy transfers small compared to the incident and scattered photon energies, $E_i \approx E_f$ and $|\mathbf{k}_i| \approx |\mathbf{k}_f|$, it is easy to show, from the simple kinematic problem, that a given scattering angle θ_s completely determines the magnitude of the momentum transfer, Q, independently of the energy transfer, E:

$$\frac{Q}{k_i} = 2\sin\left(\frac{\theta_s}{2}\right) \tag{3}$$

This is just the case of X-ray scattering from phonon-like excitations, thus not having limitations in energy transfer at a given momentum transfer. The third axis is provided by the analyzer crystal, whose role is the determination of the energy E_f of the scattered photons.

The most common way to obtain a highly monochromatic X-ray beam from a white source is [6] using a high-order Bragg reflection from a perfect crystal [so perfect that $(\Delta d/d) << (\Delta E/E) \approx 10^{-7}$]. The photoelectric absorbtion effect poses a limit in the higher order effectively usable: if we do not want further reductions of the flux we must at least take care the photoelectric absorbtion length to be larger than the extinction length due to the reflection process itself, otherwise we would lose a lot of photons by the first channel. For both the monochromator and the analyzers, we then use perfect silicon crystals [7] at the maximum reflection of (13,13,13).

In order to always optimize the fluxes, an important aspect of the beamline working is having devoted the degrees of freedom of spectrometer geometry to this purpose. From the differentiation of Bragg's law, one obtains a contribution to the relative energy resolution due to the angular divergence $\Delta\theta$ of the beam impinging on the crystal: $\Delta E/E = \Delta\theta\cot(\theta_B)$. To reach the intrinsic energy resolution of

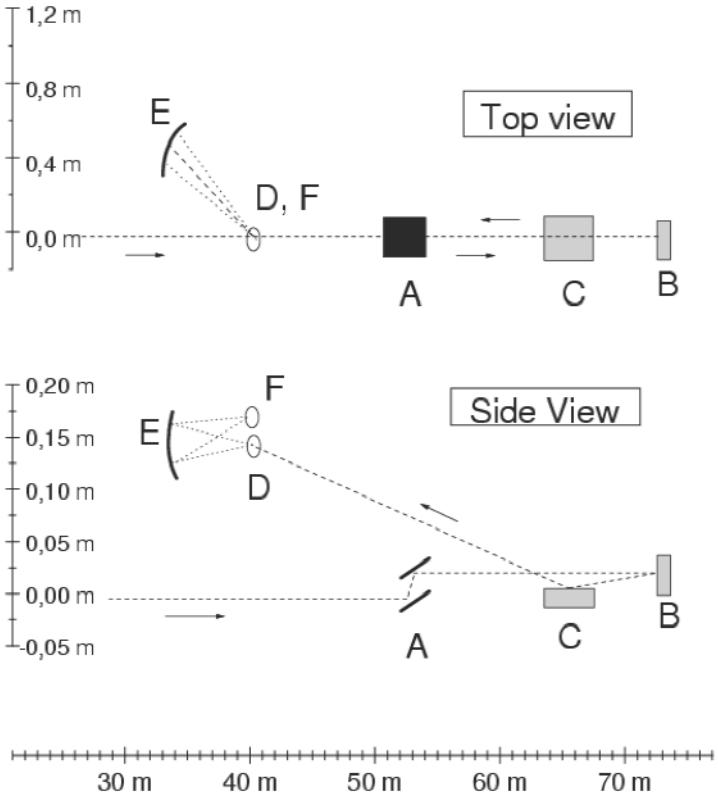

Fig. 1 Schematic layout of the inelastic X-ray scattering beamline ID16-BL21 at ESRF. The different components and their function are sketched in the figure: (A) premonochromator; (B) main monochromator; (C) toroidal mirror; (D) scattering center (sample); (E) analyzer crystal; (F) detector.

the considered reflection, it is necessary to keep $(\Delta E/E)_{\mathbf{h}} \leq \Delta\theta\cot(\theta_B)$. In typical Bragg reflection geometry $\cot(\theta_B) \approx 1$, and, for high-order reflections with $(\Delta E/E)_{\mathbf{h}} \approx 10^{-8}$, the required angular divergence should be in the 10^{-8} rad range, i.e., values much smaller than the collimation of X-ray beams available even at the new third-generation synchrotron radiation sources (10^{-5} rad). This geometrical configuration would induce a dramatic reduction of the number of photons Bragg reflected from the monochromator and analyzer crystals within the desired spectral bandwidth. An elegant way to overcome this problem is working in an extreme back-scattering geometry, i.e., the use of Bragg angles very close to 90°. In this way, the small values of $\cot(\theta_B)$ [$\theta_B \approx 89.98°$ gives $\cot(\theta_B) \approx 10^{-4}$], which allows acceptable values of $\Delta\theta$ up to above 10^{-5} rad, and therefore they become even larger than the divergence $\approx 10^{-5}$ rad of typical synchrotron radiation from an undulator source.

Although the requirements on the energy resolution of the monochromator and of the analyzer are the same, the necessary angular acceptances are very different. The X-ray beam incident on the monochromator has the angular divergence of the X-ray source, and therefore one can use a flat perfect crystal. In the case of the analyzer crystal, however, the optimal angular acceptance is dictated by the desired momentum resolution. Considering values of ΔQ in the range of 0.5 nm^{-1}, reasonable in the region of exchanged momenta of 1 to 10 nm^{-1}, the corresponding angular acceptance of the analyzer crystal must be ≈10 mrad or higher, which is again an angular range well above the acceptable values even close to back-scattering geometries. A solution consists in arranging a large number of undistorted perfect flat crystals on a spherical surface. This method has been utilized in the construction of the ESRF spectrometer on ID16: namely, approximately 10 000 silicon perfect crystals of surface size

0.7×0.7 mm^2 and thickness 3 mm have been glued on a spherical substrate of 6500-mm radius. This "perfect silicon crystal with a spherical shape" is the meV energy resolution analyzer of the BL21-ID16 beamline.

To maintain the back-scattering geometry for any energy transfer, a certain energy difference between analyzer and monochromator is obtained by keeping the Bragg angle constant, and by changing the temperature of the monochromator respective to that of the analyzer. This has the effect of varying the relative lattice parameter, and therefore the value of the reflected energies. Considering that $\Delta d/d = \alpha\Delta T$, with $\alpha = 2.56 \cdot 10^{-6}$ K^{-1} in silicon at room temperature, in order to obtain an energy step of about one-tenth of the energy resolution, i.e., $\Delta E/E \approx 10^{-9}$, it is necessary to control the monochromator crystal temperature with a precision of about 0.5 mK, throughout a temperature bath controlled with an active feedback system.

The X-ray beam from the undulator odd-harmonics has an angular divergence of approximately 15×40 μrad full width at half maximum (fwhm), a spectral bandwidth $\Delta E/E \approx 10^{-2}$, and an integrated power within this divergence of the order of 200 W. This beam is first premonochromatized to $\Delta E/E \approx 2 \cdot 10^{-2}$ using a Si(111) double crystal device kept in vacuum and at the cryogenic temperature of ≈120 K (element A in Fig. 1). The photons from the premonochromator reach the high-energy resolution back-scattering monochromator (element B in Fig. 1). This is a flat symmetrically cut silicon crystal oriented along the (111) direction, at a temperature controlled with a precision of 0.2 mK in the 285–295 K temperature region. The Bragg angle on the monochromator is $\theta_B = 89.98$. The monochromatic beam impinges on a focusing toroidal mirror (element C in Fig. 1), which gives at the sample (element D in Fig. 1) a beam size of 150(vertical) × 350(horizontal) μm^2 FWHM. The analyzer system (element E in Fig. 1) is made of an entrance pinhole, slits in front of the analyzer crystal to set the desired momentum resolution, the analyzer spherical crystal in back-scattering geometry ($\theta_B = 89.98.$), an exit pinhole in front of the detector, and the detector itself (element F in Fig. 1). There are, in fact, five independent analyzer systems with a fixed angular offset in the scattering plane among themselves. They are mounted on a 7-m-long arm which can rotate around a vertical axis passing through the scattering sample. This rotation allows us to determine the scattering angle θ_S for each of the five analyzers, and therefore the corresponding exchanged momentum. The arm operates between 0° and 15°. The spherical analyzer crystals are kept at constant temperature with a precision of 0.2 mK, and operate at the same reflection of the monochromator in Rowland circle geometry with 1:1 magnification. The detectors are inclined silicon diodes with an equivalent thickness of 2.5 mm.

The resolution performance of any of the five spectrometer channels depends on the selected Si (h h h) reflection of monochromator and analyzer, with typical values of 1.5 meV achieved when one utilizes the Si(11 11 11) reflection [8] as in the examples discussed in this work. At this order, the angular offset between the five analyzers corresponds to an exchanged momentum difference of 3 nm^{-1}. The instrumental response function of one of the five channels is reported in Fig. 2. This has been obtained by measuring the scattering from a disordered sample of Plexiglas at a Q-transfer corresponding to $Q = Q_m = 10$ nm^{-1}, and at $T = 20$ K, in order to maximize the elastic contribution to the scattering.

Finally, we want to underline that the IXS cross-section is highly coherent, contrary to neutrons where sometime it is necessary to separate "a posteriori" the coherent (genuine collective part), $\propto S(Q,E)$, from the incoherent (single particle), $\propto S_S(Q,E)$. Other remarkable advantages are related to the multiple scattering processes, in general strongly suppressed by the photoelectric absorption process and to the possibility of having very small beam sizes on the sample allows to study systems available in small quantities and/or their investigation in extreme thermodynamic conditions. Therefore, the inelastic X-ray scattering technique can be very useful and complementary to INS, although by no means can be viewed as an alternative to the powerful neutron methodologies. In particular, in the following we will show how the IXS allows the observation of an extremely important region of the E–Q plane as previously discussed, in particular, to that of the small Q-values, where the acoustic excitations, still present, are found to have energies which are not of easy access to neutrons [5].

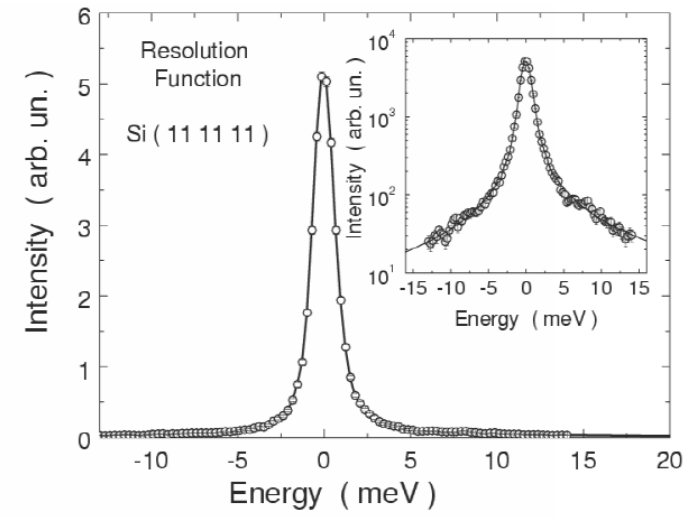

Fig. 2 Resolution function of the whole instrument obtained using the monochromator and analyzer Si(11 11 11) reflections in back-scattering geometry and measuring the elastic scattering from a plastic sample. The solid line is a Lorentzian fit to the data, used to determine the fwhm of the resolution function (1.5 ± 0.2 meV). In the inset, the same data are reported in logarithmic scale to better appreciate the shape of the tail of the resolution function.

AN EXAMPLE: THE CASE OF LIQUID GLYCEROL

As an example of useful application of the IXS technique to molecular liquids, we now present the results obtained from the prototype glass-forming glycerol. This compound (1,2,3-propanetriol, $C_3H_8O_3$) is a molecular viscous liquid that can be very easily supercooled without crystallization below its melting temperature (T_m = 291 K) and consequently can be very easily glassified at the glass-transition temperature of T_g = 186 K. The study of its high-frequency density fluctuations is therefore of crucial importance for the understanding of general aspects of microscopic dynamics in the liquid state.

High-purity anhydrous glycerol has been purchased from Aldrich. The sample has been loaded into a 20-mm-long pyrex cylindrical cell capped by 1-mm-thick diamond windows with a 4-mm opening. Due to the highly hydrophilic behavior of glycerol, the cell was loaded inside an argon glove box. For the high-temperature measurements we used a similar setup based on a 20-mm-long nickel cylinder closed by two sapphire windows (1 mm thick, 8 mm diameter), sealed on the metal with a gold welding: the cylinder has been filled through a pirex tube welded to the metal, inside the glove box, and then closed with the flame. The cell has been heated up in a standard oven working by an omega-shape resistance operating in vacuum.

In Fig. 3, we show a typical IXS spectra taken at the exchanged momentum value Q = 3 nm^{-1} in the liquid phase of the sample (T = 292 K). As can be seen from the figure, the spectrum is characterized by a huge central elastic line whose broadening reflects the relevance of relaxation processes on this frequencies: neglecting the possibility of "microscopic" relaxations [10] acting on this time scales the main role is played, as already said, by structural relaxation, therefore we can measure this characteristic time from the broadening of the central peak: in fact, as the measured intensity is the convolution of the spectrum with the instrument resolution, such measurement is possible only when the inverse of the relaxation time is comparable with the resolution width; contrarily, when the relaxation is frozen on much slower time scales, this broadening is only due to the experimental resolution. On both sides of the elastic line, we clearly observe [inset (a) in Fig. 3] the presence of an inelastic signal associated to the existence of longitudinal acoustic collective modes still surviving in the system at these length scales as predicted from several numerical simulations in other liquids [3,4].

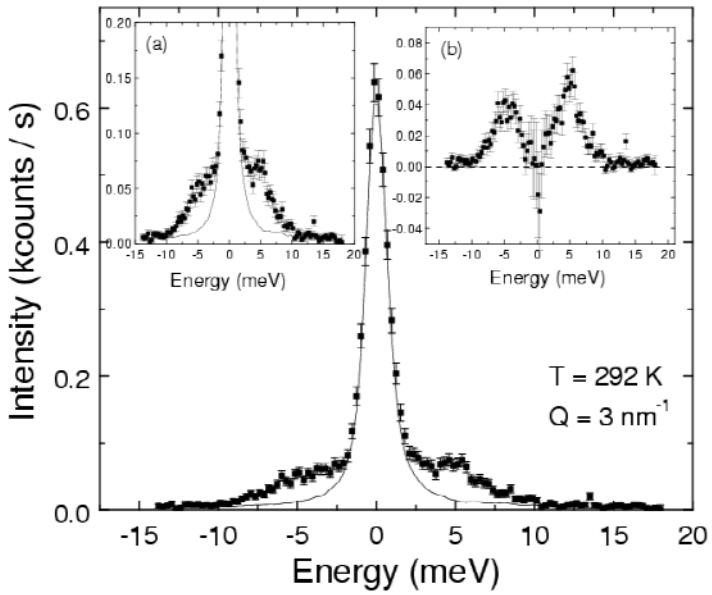

Fig. 3 A typical inelastic spectrum of glycerol is shown in the figure with the experimental resolution function rescaled for an arbitrary factor (solid line). In the inset (a) the vertical scale is expanded to emphasize the inelastic signal. In the inset (b) the subtraction of the resolution function to the spectrum is shown: two modes are clearly visible.

The inset (b) evidences the presence of well-defined inelastic peaks at a certain energy: the figure has been obtained by subtracting the simple experimental resolution (solid line in the main panel), rescaled for an arbitrary factor, to the spectrum. Obviously, this subtraction procedure contains a high degree of arbitrariness due to the much higher intensity of the central peak in respect to the inelastic signal that may cause inaccuracy in the spectral shape: in order to obtain quantitative information we must adopt a more detailed fitting procedure. For this reason, the data have been fitted by the convolution of the experimental resolution function with a classical model function, weighted by the detailed balance function to take into account for quantum effects of Bose–Einstein statistic (still relevant at this temperature as can be seen from the asymmetry of the inelastic signal). The model function is composed by the sum of two contributions:

(1) The central line is modeled by a delta-function when the broadening of the central peak is negligible; otherwise, it has been used a typical Cole–Davidson (CD) function: this function also allow us to estimate, as fitting parameter, the relaxation time and a stretching parameter which measure the deviation from a pure exponential relaxation process.

(2) The inelastic signal is modeled by a damped harmonic oscillator (DHO) function [9] to account for the longitudinal mode and determine, as fitting parameters, the energy position [$\Omega(Q)$] and broadening [$\Gamma(Q)$] of the peak.

With this procedure it is possible to analyze a set of different Q values (1–5 nm^{-1}) to get an insight into the nature of the mode. In Fig. 4, we show the spectra and the fit results: the propagating character of the excitation is quite evident. The fit results are reported in Fig. 5 where the Q dependence of fitting parameters is shown. The energy of the excitation increases linearly with increasing Q with a dispersion characterized by a sound velocity of ca. 2900 m/s. This value is in agreement with the values of c_∞ measured by Brillouin light-scattering technique at this temperature [11]. This behavior is just what we should expect from the fact that at this temperature we don't appreciate a broadening of the central line, i.e., the dotted line in Fig. 4 is the experimental resolution convoluted with a delta-func-

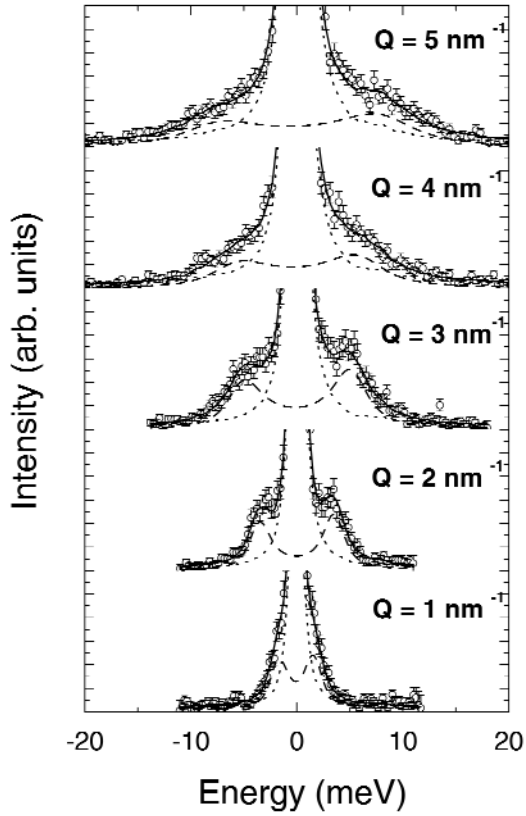

Fig. 4 This figure shows the spectra at different Q values. The fit results are also shown (solid line) and the two contributions to the model function, elastic (dotted line) and inelastic (dashed line) are also reported.

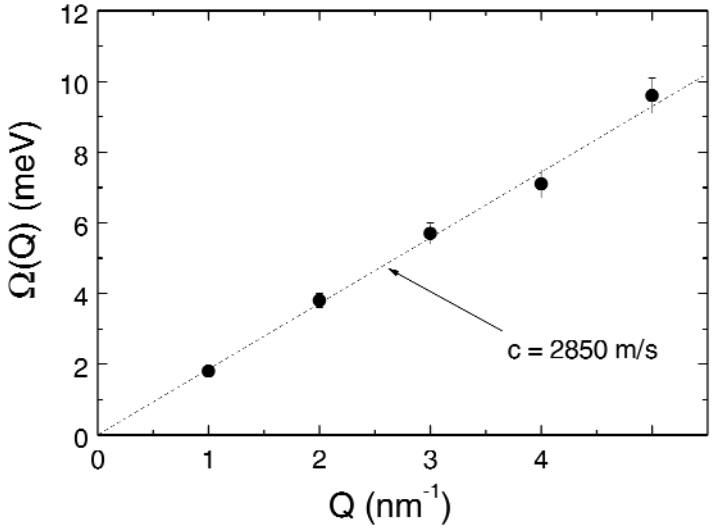

Fig. 5 The figure shows the Q dependence of the inelastic peak energy position (full dots): the dashed line shows the linear behavior correspondent to a sound velocity of 2850 m/s.

tion: this means that our frequency range is much higher than the inverse of the structural relaxation time at this temperature, the structural degrees of freedom appear as frozen, and the liquid exhibits a solid-like response as evinced from the sound velocity value.

Figure 6 represents the attenuation of the inelastic excitations in a log–log scale: from the fits a Q^2-dependence is reported, according with low Q range BLS measurements and with the hydrodynamic behavior [1,11]. The origin of the attenuation mechanism, far from any structural effect, is supposed to mainly lie in the topological microscopic disorder of the liquid structure which does not allow a plane wave description of the system: Q is no more a good quantum number and the excitation assumes a finite life-time; the anharmonicity also starts to contribute to the attenuation at these temperatures, as can be seen from the monotonic temperature dependence of Γ [14].

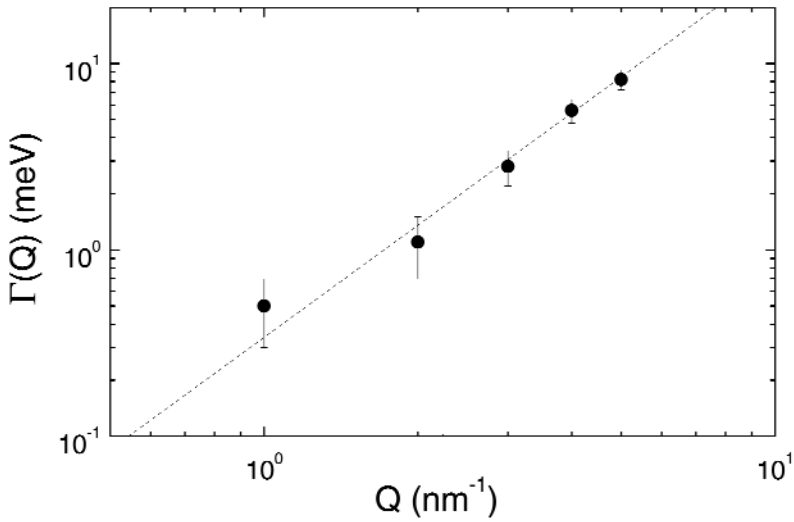

Fig. 6 In a log–log scale is shown the Q-dependence of the acoustic attenuation: the dashed line emphasizes its full consistence with a Q^2-increasing.

Finally, we want to turn our attention again to the evidence of structural relaxation on these energy scales: as already pointed out, no effects in the range covered by IXS technique can be observed at ambient temperature. In this temperature range, instead, both light-scattering (line) [12] and viscosity (open dots) [13] data provide us the temperature dependence of the structural relaxation time. As clearly shown, indeed, at T = 292 K, the inverse of the relaxation time is four orders of magnitude smaller than our frequency range and so not directly measurable. Viscosity data show on the other side how increasing temperature the time scales of the structural relaxation should approach our frequency window. In order to verify this prediction and then to measure its characteristic time, we performed a study of the spectra in the temperature range 170–560 K. The data reported in the following therefore illustrate the utility of the IXS technique in the study of the structural relaxational dynamics of glass-forming systems.

Figure 7 shows the spectra at different selected temperatures at the Q value of 17 nm^{-1}: the figure emphasizes the behavior of the elastic line, a discussion about the effects of the temperature increasing on the inelastic signal and on the value of the sound velocity, which can be found elsewhere [14]. The elastic peak broadening is not appreciable in respect to the experimental resolution (dotted line) up to 373 K; in the higher-temperature spectra, instead, a consistent broadening can be estimate from a Cole–Davidson fit of the central peak as explained before. In Fig. 8, we report the results for the

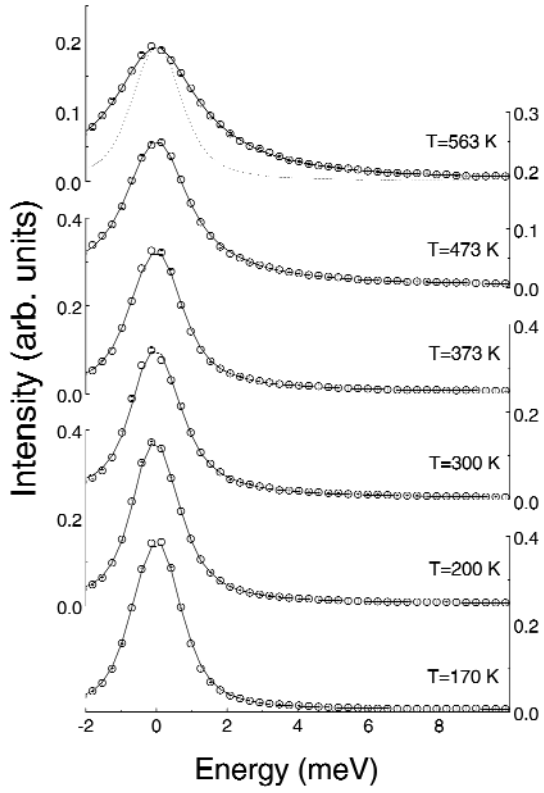

Fig. 7 In the figure the elastic line of the spectra (dots) is shown at different temperatures; the fits result is also reported (solid line) together with the experimental resolution to emphasize the peak broadening.

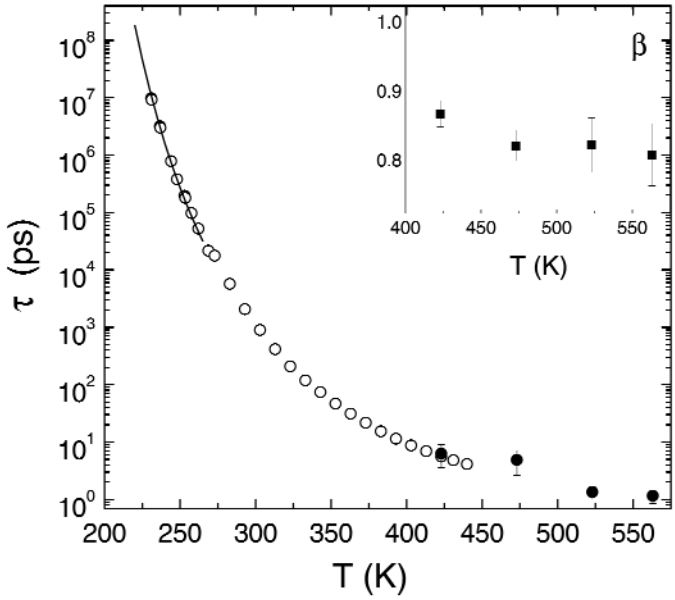

Fig. 8 Values of the structural relaxation time in glycerol as function of temperature. Full dots: this work (central peak broadening). Full line: light scattering. Open dots: viscosity data scaled by an arbitrary factor. Inset: values of the stretching exponent of the Cole–Davidson function.

fitting parameters of the Cole–Davidson function. The relaxation time τ is in excellent agreement with the available measurements in a range extended up to 563 K. Moreover, a quite strong deviation from a pure exponential relaxational behavior is emphasized by the values of the stretching parameter β, reported in the inset, progressively deviating from the unit at increasing temperatures.

REFERENCES

1. U. Balucani and M. Zoppi. *Dynamics of the Liquid State*, Oxford Science Publishing, Oxford, (1994).
2. BLS spectroscopy allows the study of the $S(Q,\omega)$ up to Q values of the order of 0.04 nm^{-1}, i.e., well within the expected range of validity of the hydrodynamic theory.
3. W. E. Alley, B. J. Alder, S. Yip. *Phys. Rev.* **A27**, 3174 (1983); C. Bruin, J. P. J. Michels, J. C. Van Rijs, L. A. deGraaf, I. M. deSchepper. *Phys. Lett.* **110A**, 40 (1985).
4. I. M. deSchepper, J. C. Van Rijs, A. A. vanWell, P. Verkerk, L. A. de Graaf. *Phys. Rev. A* **29**, 1602 (1984); U. Bafile, F. Barocchi, M. Neumann, P. Verkerk. *J. Phys. Cond. Matt.* **6**, A107 (1994).
5. F. Sette, G. Ruocco, M. Krisch, U. Bergmann, C. Masciovecchio, V. Mazzacurati, G. Signorelli, R. Verbeni. *Phys. Rev. Lett.* **75**, 850 (1995); G. Ruocco, F. Sette, M. Krisch, U. Bergmann, C. Masciovecchio, V. Mazzacurati, G. Signorelli, R. Verbeni. *Nature* **379**, 521 (1996); F. Sette, G. Ruocco, M. Krisch, C. Masciovecchio, R. Verbeni, U. Bergmann. *Phys. Rev. Lett.* **77**, 83 (1996); T. Scopigno, U. Balucani, A. Cunsolo, C. Masciovecchio, G. Ruocco, F. Sette, R. Verbeni. *Europhys. Lett.* **50**, 189 (2000); T. Scopigno, U. Balucani, G. Ruocco, F. Sette. *Phys. Rev. Lett.* **85**, 4076 (2000); T. Scopigno, U. Balucani, G. Ruocco, F. Sette. *J. Phys. C* **12**, 8009 (2000); T. Scopigno, U. Balucani, G. Ruocco, F. Sette. *Phys. Rev. E* **63**, 011210 (2001); T. Scopigno, A. Filipponi, M. Krisch, G. Monaco, G. Ruocco, F. Sette. *Phys. Rev. Lett.* **89**, 255506 (2002).
6. H. Zachariasen. *Theory of X-ray Diffraction in Crystals*, Dover, New York (1944).
7. R. Verbeni, F. Sette, M. H. Krisch, U. Bergmann, B. Gorges, C. Halcoussis, K. Martel, C. Masciovecchio, G. Ruocco, H. Sinn. *J. Synch. Rad.* **3**, 62, (1996).
8. C. Masciovecchio, U. Bergmann, M. H. Krisch, G. Ruocco, F. Sette, R. Verbeni. *Nucl. Inst. Meth.* **B-111**, 181 (1996); C. Masciovecchio, U. Bergmann, M. H. Krisch, G. Ruocco, F. Sette, R. Verbeni. *Nucl. Inst. Meth.* **B-117**, 339 (1996).
9. B. Fak and B. Dorner. Institute Laue Langevin (Grenoble, France), Technical Report No. 92FA008S (1992).
10. G. Ruocco, F. Sette, R. Di Leonardo, G. Monaco, M. Sampoli, T. Scopigno, G. Viliani. *Phys. Rev. Lett.* **84**, 5788 (2000); T. Scopigno, G. Ruocco, F. Sette, G. Viliani. *Phys. Rev. E* **66**, 031205 (2002).
11. C. Masciovecchio. Ph.D. thesis, Universita Joseph Fourier - Grenoble (France) (1998).
12. D. M. Paolucci and K. A. Nelson. *J. Chem. Phys.* **112**, 6725 (2000).
13. H. Landolt and R. Boernstein. Sec. 25-1, Vol. II/5a, VI ed.
14. C. Masciovecchio, G. Monaco, G. Ruocco, F. Sette, A. Cunsolo, M. Krisch, A. Mermet, M. Soltwisch, R. Verbeni. *Phys. Rev. Lett.* **80**, 544 (1998).